



Universiteit
Leiden
The Netherlands

Chemical tools to probe the proteasome

Verdoes, M.

Citation

Verdoes, M. (2008, December 19). *Chemical tools to probe the proteasome*. Retrieved from <https://hdl.handle.net/1887/13370>

Version: Corrected Publisher's Version

License: [Licence agreement concerning inclusion of doctoral thesis in the Institutional Repository of the University of Leiden](#)

Downloaded from: <https://hdl.handle.net/1887/13370>

Note: To cite this publication please use the final published version (if applicable).

2

A Fluorescent Broad-Spectrum Proteasome Inhibitor for Labeling Proteasomes *In Vitro* and *In Vivo*.

M. Verdoes, B.I. Florea, V. Menendez-Benito, C.J. Maynard, M.D. Witte, W.A. van der Linden, A.M.C.H. van den Nieuwendijk, T. Hofmann, C.R. Berkers, F.W. van Leeuwen, T.A. Groothuis, M.A. Leeuwenburgh, H. Ovaa, J.J. Neefjes, D.V. Filippov, G.A. van der Marel, N.P. Dantuma, H.S. Overkleeft, *Chemistry & Biology*, **2006**, *13*, 1217-1226.

2.1 Introduction

The 26S proteasome is the central protease in the ATP- and ubiquitin-dependent degradation of proteins in the eukaryotic cytoplasm and nucleus and is involved in the degradation of 80-90% of all cellular proteins. Proteasome substrates include abnormal and damaged proteins, cell-cycle regulators, oncogens and tumor suppressors, and the proteasome is imperative in the generation of MHC class I antigenic peptides.¹ Eukaryotic proteasomes contain two copies of seven distinct α and β subunits each. These subunits assemble into two types of hetero-oligomeric rings each composed of seven subunits [(α 1- α 7) and (β 1- β 7)]. The 20S proteasome is formed by two juxtaposed rings of β subunits flanked on top and bottom by a ring of α -subunits.² When capped by the 19S regulatory complex at both ends, the proteolytically active 26S proteasome is formed which is responsible for ATP-dependent proteolysis of poly-ubiquitinated target proteins.³

In the eukaryotic proteasome, three of the seven β subunits are responsible for the proteolytic activities of the proteasome. Characterization of the active β 1, β 2 and β 5 subunits led to the classification of their substrate specificity as peptidylglutamyl peptide hydrolytic (PGPH, or caspase-like), trypsin-like and chymotrypsin-like, respectively. In immune competent cells three additional active β subunits (β i) are expressed upon interferon- γ stimulation, which replace their closely related, constitutively expressed β subunits in newly formed 20S proteasome particles.²

The proteolytic subunits β 1, β 2 and β 5, and their immunoproteasomal counterparts, β 1i, β 2i and β 5i act by nucleophilic attack of the γ -hydroxyl of the *N*-terminal threonine on the carbonyl of the peptide bond destined for cleavage. The α -amine of the threonine acts as a base in the catalytic cycle. The existence and evolutionary development of six different

active β subunits, their divergent substrate specificities, and their individual roles in cellular processes constitute a vast research field of interest in both academia and the pharmaceutical industry. This scientific demand can benefit from an activity-based proteasome probe that ideally (1) specifically targets the proteasome, (2) covalently and irreversibly binds to the active β and β_i subunits indiscriminately, (3) facilitates direct, rapid, accurate, and sensitive detection, (4) is cell permeable, and (5) enables monitoring of the proteasome by microscopic techniques in living cells. To date, none of the available activity-based proteasome probes meet all of these requirements.^{4,5} The compound that comes closest is the radiolabeled proteasome inhibitor $\text{AdaY}^{(125\text{I})}\text{Ahx}_3\text{L}_3\text{VS}$ (**1**, Figure 1).⁶ This inhibitor is selective for the proteasome, labels the β subunits with equal intensity, and enables accurate and sensitive in-gel detection. However, usage of this activity-based probe is restricted to *in vitro* applications since this compound is not cell permeable. Recently, the weakly fluorescent and cell-permeable proteasome inhibitor dansylAhx₃L₃VS (**2**) was developed for profiling proteasome activity in living cells, enabling readout by anti-dansyl immunoblotting.⁷ The low quantum yield and near-UV excitation of the dansyl makes this compound unsatisfactory for in-gel detection and standard fluorescence microscopic techniques.

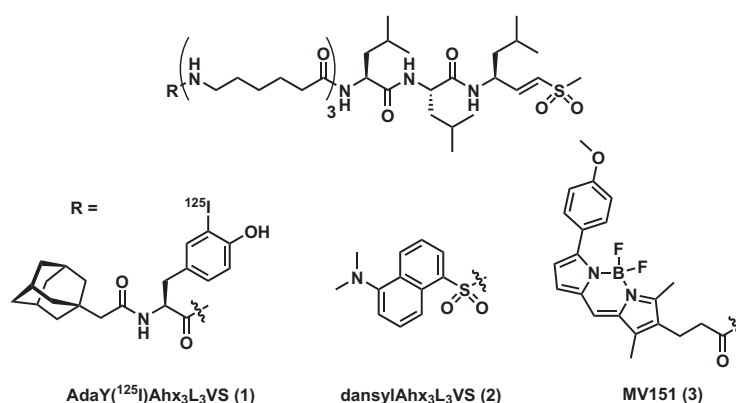


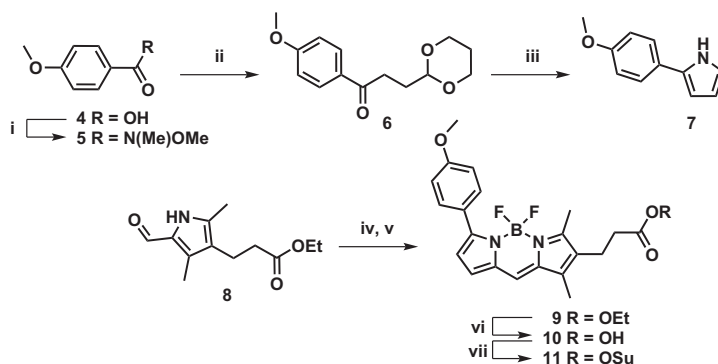
Figure 1. The proteasome probes $\text{AdaY}^{(125\text{I})}\text{Ahx}_3\text{L}_3\text{VS}$ (**1**), dansylAhx₃L₃VS (**2**) and MV151 (**3**).

In this chapter the synthesis and characterization of the fluorescent, cell-permeable, and activity-based proteasome probe BODIPY TMR-Ahx₃L₃VS (MV151, **3**, in which BODIPY stands for boron-dipyrromethene and TMR stands for tetramethylrhodamine) is described. After proteasome labeling and protein separation by SDS-PAGE, the labeled proteasome subunits are visualized by direct in-gel fluorescence readout. This compound enables fast and sensitive labeling of proteasome activity *in vitro*, in cells, and in mice, is compatible with live-cell imaging techniques and facilitates screening and determination of the subunit specificity of novel proteasome inhibitors.

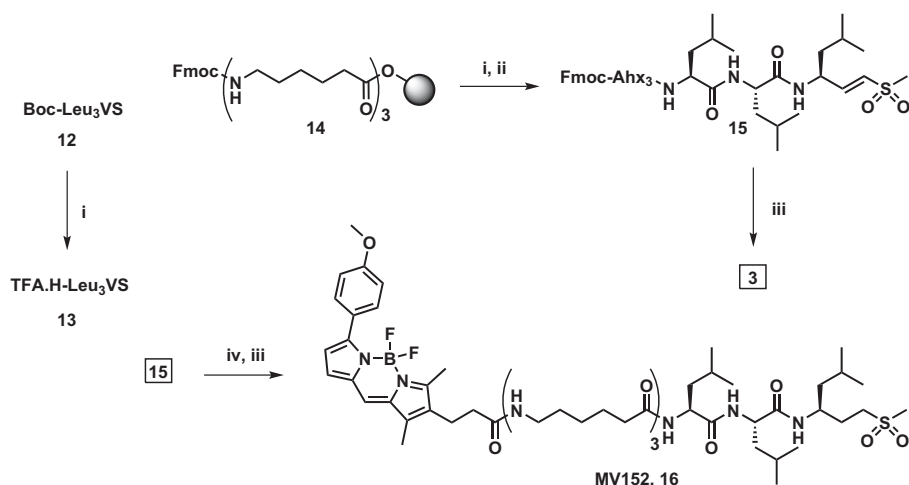
2.2 Results and discussion

A proteasome probe typically consists of three parts, being a reporter group, a peptidic recognition element and a warhead. In BODIPY TMR-Ahx₃L₃VS (MV151, **3**), the warhead is the leucine derived vinyl methyl sulfone. This Michael acceptor mimics the carbonyl of a substrate peptide bond destined to be cleaved. Nucleophilic attack of the γ -hydroxyl of the *N*-terminal threonine on the vinyl sulfone covalently links the probe to the proteolytically active β subunit and renders the protease deactivated (see Chapter 1.4 for a more detailed description). BODIPY TMR-Ahx₃L₃VS (MV151, **3**) and the inactive, negative control compound BODIPY TMR-Ahx₃L₃ES (MV152, **16**), in which the vinyl sulfone moiety is reduced to an ethyl sulfone, were synthesized as depicted in Scheme 1 and 2. The synthesis commences with the preparation of the succinimidyl ester of the fluorophore BODIPY TMR (**11**) using a modified procedure of the synthesis described in the patents for related compounds (Scheme 1).⁸⁻¹⁰ Anisic acid (**4**) was converted into Weinreb-amide **5**, which upon treatment with (1,3-dioxane-2-ylethyl)-magnesium bromide in THF yielded ketone **6**. *In situ* deprotection of the aldehyde and Paal-Knorr reaction afforded methoxy-phenyl pyrrole **7**, which was condensed with carboxyaldehyde pyrrole **8**.¹¹ Subsequent treatment of the resulting dipyrrole HBr salt with BF₃·Et₂O and triethylamine in refluxing dichloroethane afforded BODIPY TMR ethyl ester **9**. Saponification of the ethyl ester and subsequent condensation of **10** with *N*-hydroxysuccinimide furnished BODIPY TMR succinimidyl ester (**11**). Acidic cleavage of Fmoc-Ahx₃-Wang resin (**14**), synthesized employing standard Fmoc-based solid-phase peptide chemistry, gave the crude Fmoc-Ahx₃-OH, which was block coupled to TFA·H-Leu₃VS (**13**),¹² to yield Fmoc-protected hexapeptide **15** (Scheme

Scheme 1. Synthesis of BODIPY TMR-OSu **11**.



Reagents and conditions: i) HN(Me)OMe·HCl (1 equiv.), HCTU (1.1 equiv.), DiPEA (2 equiv.), DCM, 12 hr., 89%. ii) (1,3-dioxane-2-ylethyl)-magnesium bromide (1.5 equiv.), THF, 3 hr., 89%. iii) NH₄OAc (12 equiv.), Ac₂O (3.7 equiv.), AcOH, 3 hr., 70%. iv) **7**, HBr 48% in H₂O (1.5 equiv.), EtOH, 0 °C, 1 hr. v) BF₃·Et₂O (5 equiv.), TEA (3 equiv.), DCE, 90 °C, 30 min., 68% (2 steps). vi) 0.1M NaOH (1 equiv.), dioxane, 15 hr., 40%. vii) *N*-hydroxysuccinimide (4 equiv.), EDC·HCl (4 equiv.), DCM, 15 hr., 69%.

Scheme 2. Synthesis of BODIPY TMR-Ahx₃L₃VS (**3**), and the control compound BODIPY TMR-Ahx₃L₃ES (**16**).

Reagents and conditions: i) TFA/DCM 1/1 (v/v), 30 min. ii) **13** (2 equiv.), BOP (2.5 equiv.), DIPEA (6 equiv.), 12 hr., 98%. iii) (a) DBU (1 equiv.), DMF, 5 min. (b) HOBT (4.5 equiv.), 1 min. (c) **11** (1 equiv.), DIPEA (6 equiv.), 30 min., **3** 99%, **16** 88%. iv) Pd/C, H₂, MeOH, 2 hr.

2). *In situ* deprotection of the Fmoc-protecting group with DBU and treatment with BODIPY TMR succinimidyl ester (**11**) afforded the potential proteasome probe MV151 (**3**). In order to obtain the inactive control compound **16**, hexapeptide **15** was first treated with hydrogen gas and palladium on charcoal in methanol to reduce the vinyl sulfone, followed by Fmoc cleavage and introduction of the BODIPY TMR moiety.

The potency of MV151 (**3**) to inhibit the proteasome was determined in a fluorogenic substrate assay.¹³ EL-4 lysates were incubated with increasing concentrations of MV151, and the cleavage of the substrates Suc-Leu-Leu-Val-Tyr-AMC (chymotrypsin-like activity, β₅), Z-Ala-Ala-Arg-AMC (trypsin-like activity, β₂), and Z-Leu-Leu-Glu-βNA (PGPH activity, β₁) was monitored. At concentrations of 1 μM and higher, MV151 completely inhibits all three activities. Below a 1 μM concentration, MV151 appears to inhibit the trypsin-like activity and the chymotrypsin-like activity more efficiently than it inhibits the PGPH activity (Figure 2A). This might be due to differences in activity between the subunits, to allosteric effects, to minor subunit specificities of the probe, or to nonsaturation kinetics. Having established the proteasome inhibitory capacity, direct in-gel visualization of MV151-labeled proteasome subunits was explored by using a fluorescence scanner. Treatment of purified human 20S proteasome with MV151 showed uniform labeling of the active subunits β₁, β₂, and β₅ (Figure 2B). To determine the sensitivity of the in-gel detection, the fluorescence readout of the gel (Figure 2B) and the detection of proteasome subunits by silver staining (Figure 2C) was directly compared. The in-gel detection proved to be very sensitive since as little as 3 ng proteasome was sufficient to detect individual MV151-labeled proteasome

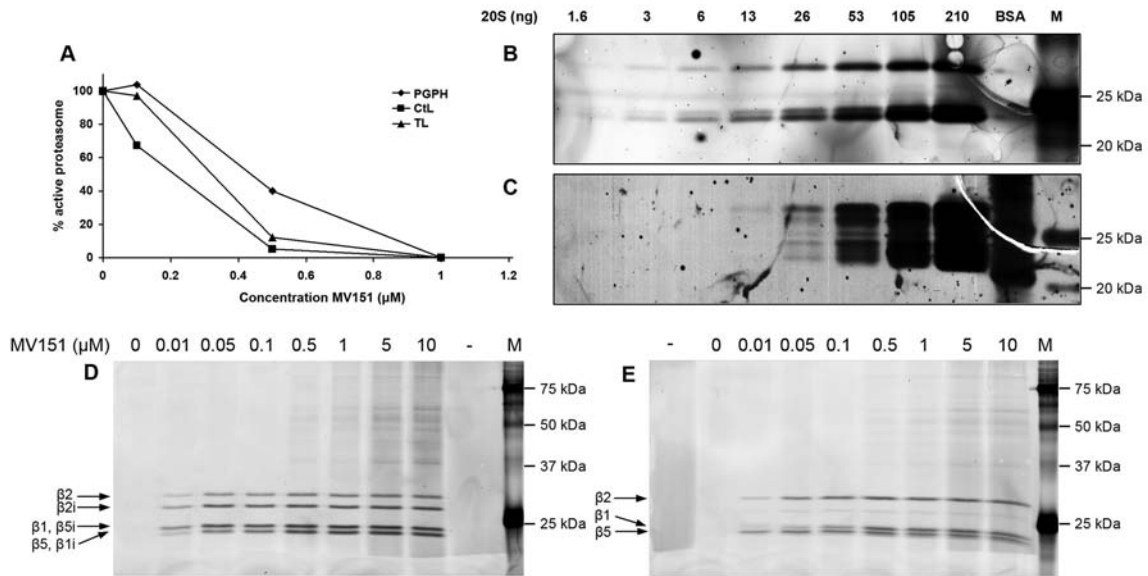


Figure 2. Proteasome labeling and in-gel detection from cell extracts.

(A) Measurement of proteasome activity with fluorogenic substrates after treatment of EL-4 lysates with the indicated concentrations of MV151 (3) (PGPH = peptidylglutamyl peptide hydrolytic activity, CtL = chymotrypsin-like activity, TL = trypsin-like activity). (B,C) Comparison between fluorescent in-gel detection and silver-staining. The indicated amounts of purified human 20S proteasome were incubated for 1 hr. at 37 °C with 300 nM MV151, resolved by SDS-PAGE and detected by (B) direct fluorescence in-gel read-out and by (C) silver staining. (D,E) Proteasome labeling profile in (D) EL-4 and (E) HeLa lysates (10 µg total protein) incubated for 1 hr. at 37 °C with the indicated concentrations of MV151. "M" represents the molecular marker (Dual Color, BioRad), "-" represents heat-inactivated lysates, incubated with 10 µM MV151 for 1 hr. at 37 °C.

subunits. In-gel detection of fluorescently labeled proteasome subunits is at least three times more sensitive than silver staining. To compare the labeling of the constitutive subunits β_1 , β_2 , and β_5 with that of the immunoproteasome β_{1i} , β_{2i} , and β_{5i} subunits, lysates of the human cervix carcinoma cell line HeLa (expressing constitutive proteasome) and the murine lymphoid cell line EL-4 (expressing both constitutive and immunoproteasome) were treated with increasing concentrations of MV151. All active constitutive and inducible β proteasome subunits were neatly and uniformly labeled by MV151 (Figures 2D and 2E). All subunits were already detectable at a concentration of 10 nM MV151 and reached saturation in fluorescence signal at 1 µM MV151. At higher concentrations of MV151, an increased nonspecific labeling was observed in the high molecular weight region.

Next, a set of competition experiments versus MV151 was performed to determine the potency and subunit specificity of a panel of known proteasome inhibitors (Figure 3). EL-4 and HeLa cell lysates (10 µg total protein) were exposed to the inhibitor of interest for 1 hr. After incubation with the proteasome inhibitor, the subunits that were still active were fluorescently labeled by treating the lysates with 100 nM MV151 for 1 hr. The proteins were

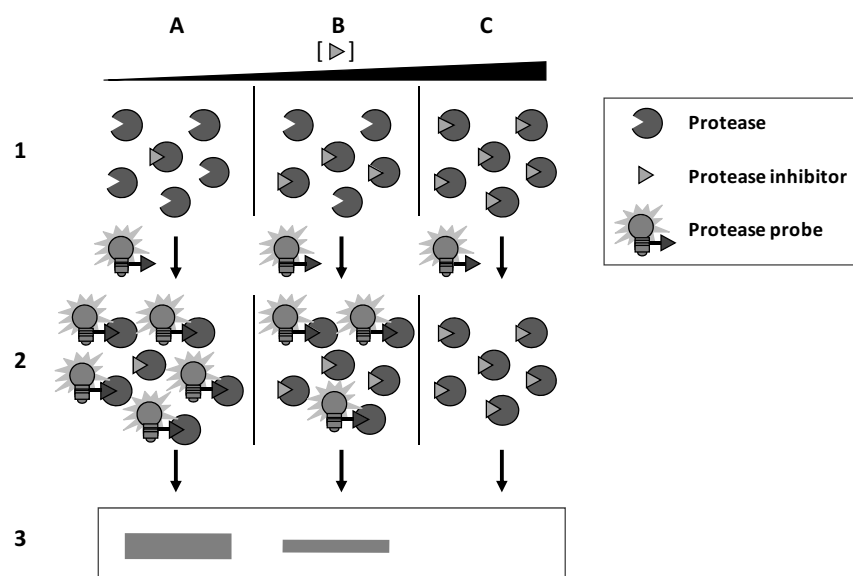


Figure 3. Schematic representation of a competition experiment.

Samples **A** to **C** are exposed to increasing concentrations of an inhibitor of interest in step **1**. In step **2** the residual protease activity is labeled with a fluorescent probe. Step **3** entails SDS-PAGE and fluorescence readout of the resulting gel. The more potent the inhibitor of interest, the sooner the fluorescent bands will disappear.

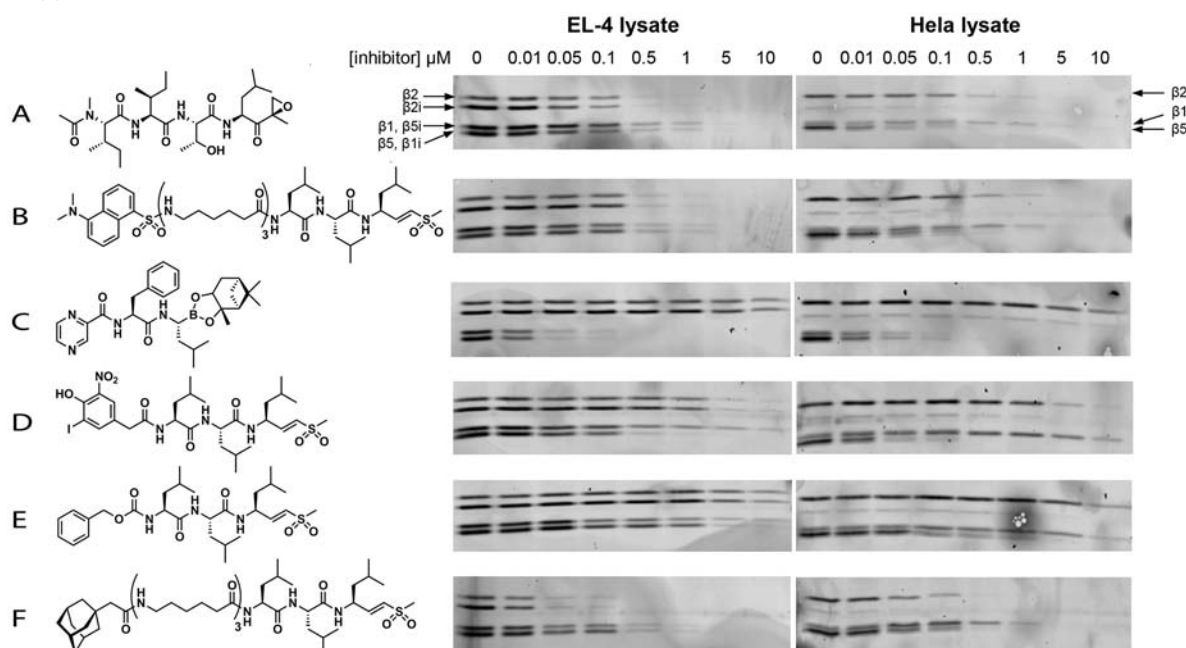


Figure 4. Proteasome profiling screen of known inhibitors using MV151.

(A-F) EL-4 and HeLa lysates (10 μg total protein) were incubated with the indicated concentrations of the proteasome inhibitor (A) epoxomicin, (B) dansylAhx₃L₃VS, (C) bortezomib pinanediol boronic ester, (D) NIP-LVS (E) Z-LVS and (F) AdaAhx₃L₃VS for 1 hr. at 37 °C. Residual proteasome activity was fluorescently labeled by incubation with 0.1 μM MV151 for 1 hr. at 37 °C.

separated on SDS-PAGE and the gels were scanned on a fluorescence scanner. In HeLa lysates, epoxomicin preferentially inhibits the β 5 subunit, already visible at a 10 nM

concentration (Figure 4A, right panel). At epoxomicin concentrations over 100 nM, β_1 and β_2 are also targeted, with a slight preference for β_2 (at 5 μ M epoxomicin, β_2 fluorescence is absent and a faint band of β_1 is still visible). This is in accordance with the inhibition profile of epoxomicin determined with purified 20S proteasome.¹⁴ Interestingly, in EL-4 lysates, epoxomicin preferentially inactivates β_2 and β_{2i} and is less active toward constitutive and immunoinduced β_1 and β_5 subunits (Figure 4A, left panel). DansylAhx₃L₃VS⁷ inhibits all active constitutive and immunoinduced subunits in EL-4 from concentrations of 500 nM and greater (Figure 4B, left panel). In HeLa lysates, dansylAhx₃L₃VS has a preference for the β_5 subunit, which is visible at 100 nM, and less of a preference for the β_1 and β_2 subunits, which are visible at slightly higher concentrations (Figure 4B, right panel). The dipeptidyl pinanediol boronic ester (pinanediol boronic ester of bortezomib¹²) shows a strong selectivity for the constitutive β_1 and β_5 subunits in HeLa lysates (Figure 4C, right panel) and β_1 , β_{1i} , β_5 , and β_{5i} in EL-4 lysates (Figure 4C, left panel). The inhibition profile of the dipeptidyl pinanediol boronic ester is comparable to the labeling profile of bortezomib, with potency in the same order of magnitude.⁷ As previously reported, NIP-LVS¹² shows a predilection for β_5 (Figure 4D), whereas Z-LVS¹² (Figure 4E) proves to be the least potent compound and shows some preference for the constitutive and immunoinduced β_1 and β_5 subunits. In EL-4 lysates, AdaAhx₃L₃VS⁶ first targets the β_2 and β_{2i} subunits, and it shows a preference for β_2 and β_5 in HeLa lysates (Figure 4F). Altogether, this experiment shows that MV151 can be used for the determination of inhibition profiles of proteasome inhibitors. Exploiting the sensitivity of in-gel detection of MV151, it is possible to demonstrate that the inhibitors tested show subtle differences in the proteasome inhibition profile.

The capacity of MV151 to cross the cell membrane and label proteasome subunits in living cells was determined in the following experiment. Living EL-4 and HeLa cells were incubated with increasing concentrations of MV151 for 2 hr., before the cells were harvested, washed and lysed. Specific and sensitive labeling of all proteasome subunits was observed in EL-4 (Figure 5A) and HeLa cells (Figure 5B), although higher concentrations were required than for labeling of subunits in lysates. Labeling of the β_1 subunit shows a lower intensity than in lysates, whereas β_5 labeling looks more pronounced. This difference in the labeling profile between the proteasome in cell lysates and living cells has been previously reported,⁷ however, the reason for this remains unclear. Importantly, incubation of EL-4 and HeLa cells with the inactive control compound MV152 (**16**), which is almost identical to MV151 but lacks the reactive vinyl sulfone warhead, showed no labeling of the proteasome or any other protein (Figures 5A and 5B).

To confirm the ability of MV151 to inhibit proteasome activity in living cells, HeLa cells stably expressing a green fluorescent protein (GFP) reporter proteasome substrate¹⁶ were exposed to MV151. The ubiquitin^{G76V}-GFP fusion (Ub^{G76V}-GFP) expressed by these cells

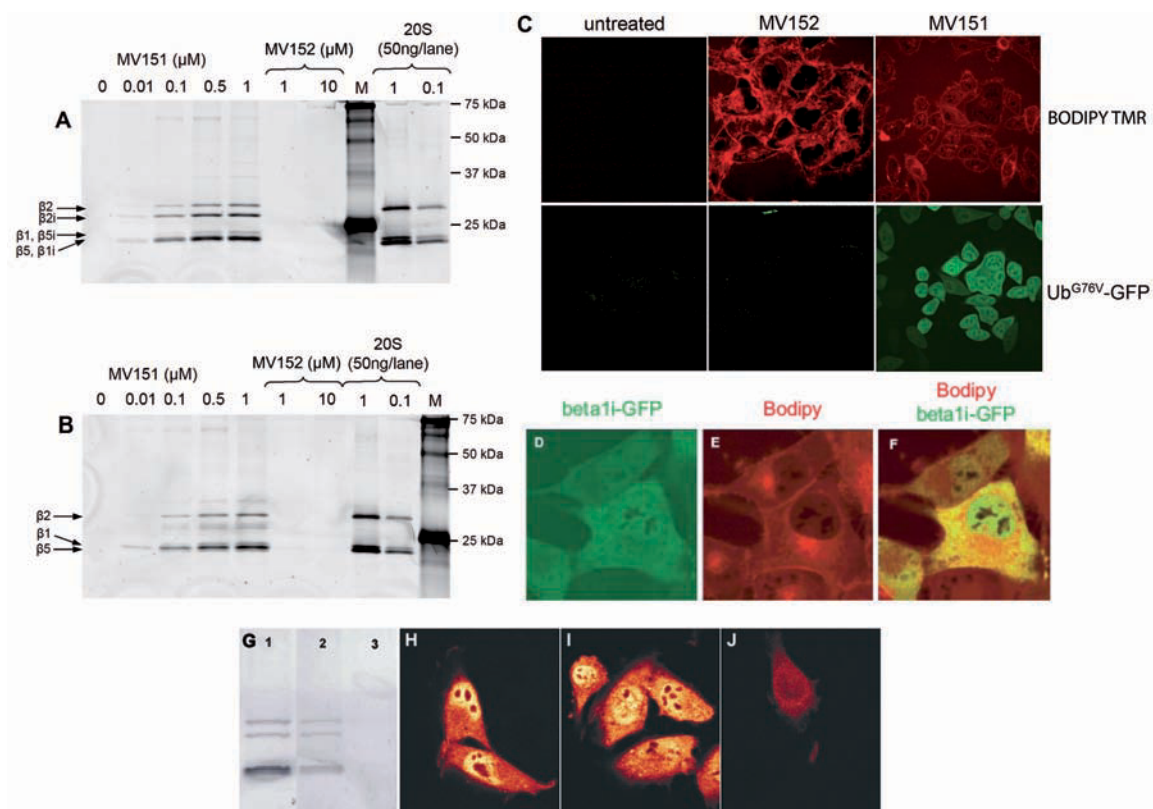


Figure 5. Functional proteasome inhibition in living cells.

(A-B) Proteasome profiling in living (A) EL-4 and (B) HeLa cells after 2 hr. incubation with the indicated concentrations of MV151. As a control, the cells were incubated with the inactive compound MV152. Purified 20S proteasome labeled with MV151 is also shown. (C) Representative micrographs of Ub^{G76V}-GFP HeLa cells that were untreated (left panel), incubated for 12 hr. with 10 μM inactive MV152 (middle panel), and 10 μM MV151 (right panel). BODIPY TMR and Ub^{G76V}-GFP fluorescence are shown. (D-F) Colocalization of GFP-labeled proteasome and MV151 in living GFP-β1i MelJuSo cells treated for 8 hr. with 10 μM MV151. (D) GFP-β1i, (E) BODIPY TMR fluorescence and (F) merged are shown. (G) In-gel visualization of proteasome labeling in living EL-4. Lane 1: 1 hr. incubation with MV151 (250 nM). Lane 2: 1 hr. incubation with MV151 (250 nM) followed by 1 hr. incubation with MG132 (5 μM). Lane 3: 1 hr. incubation with MG132 (5 μM) followed by 1 hr. incubation with MV151 (250 nM). (H-J) CLSM pictures of BODIPY TMR fluorescence in MelJuSo Ub-R-GFP cells after formaldehyde fixation, gain 700. (H) 1 hr. incubation with MV151 (500 nM). (I) 1 hr. incubation with MV151 (500 nM) followed by 1 hr. incubation with MG132 (5 μM). (J) 1 hr. incubation with MG132 (5 μM) followed by 1 hr. incubation with MV151 (500 nM).

is normally rapidly degraded by the proteasome. When the proteasome is blocked however, the reporter will accumulate and increased GFP fluorescence can be seen. Indeed, untreated HeLa cells emitted only low GFP fluorescence (Figure 5C, left panel). Cells that were exposed to 10 μM of the inactive MV152 for 12 hr. did accumulate the control compound, but they did not show increased levels of GFP fluorescence (Figure 5C, middle panel). During 12 hr. of exposure to 10 μM MV151, cells accumulated the inhibitor and showed significantly increased levels of GFP fluorescence (Figure 5C, right panel). Strong

BODIPY TMR fluorescence is apparent in the membranous compartments of cells treated with the inactive MV152. This fluorescence, which appears to be stronger than in MV151-treated cells, and which is not due to proteasome labeling (as judged from SDS-PAGE analysis), is due to accumulation of MV152 in the hydrophobic environment of the membranes. The active MV151 is likely to accumulate in the lipid bilayers to a lesser extent, because it is sequestered by the proteasome active sites. There was no visual evidence of cellular toxicity at the dose and exposure time used in this study. These results were confirmed by a study with the human melanoma cell line MelJuSo stably expressing the N-end-rule reporter proteasome substrate Ub-R-GFP¹⁶ (data not shown). Next, it was determined whether the intracellular staining pattern of MV151 colocalized with the proteasome in living cells. To this end, a MelJuSo cell line that stably expresses a GFP-tagged β 1i proteasome subunit, which is efficiently incorporated into the proteasome particles was used.¹⁷ The GFP- β 1i fusion construct shows ubiquitous distribution throughout the cytoplasm and nucleus, with exception of nucleoli and the nuclear envelope (Figure 5D). The GFP- β 1i cells were incubated with 10 μ M MV151 and the distribution of proteasomes and probe was compared. The intracellular permeation of MV151 was monitored in time and is characterized by a fast permeation phase (several minutes), followed by a slow distribution phase (several hours). During the permeation phase, the compound showed significant association with the plasma membrane, in discrete cytoplasmic vesicular and membranous fractions and at the nuclear envelope. After 5 hours of distribution, MV151 is localized throughout the cell, with the exception of the nucleoli, similar to the GFP- β 1i fusion protein (Figures 5D-5F). The fact that MV151 is excluded from the nucleoli is in line with the idea that the compound is associated with the proteasome. In some cells, granular accumulation of MV151 was observed in the cytoplasm in close proximity to the nucleus. To attest whether the in-gel readout could be correlated with the fluorescent microscopy data, MV151 was competed with the proteasome inhibitor MG132 (ZL₃-al)¹⁸ in EL-4 cells (Figure 5G) and MelJuSo Ub-R-GFP cells (Figure 5H-J). EL-4 cells incubated with MV151 for 1 hour showed labeling of all the active proteasome subunits on gel (Figure 5G, lane 1). MelJuSo Ub-R-GFP cells treated in the same way showed, after fixation with formaldehyde, strong fluorescence in the cytoplasm and nucleus, with the exception of nucleoli (Figure 5H). Cells incubated with MV151 for 1 hour, followed by a 1 hour incubation with MG132, still showed labeling of the active proteasome subunits on gel (Figure 5G, lane 2) and a similar cellular localization to that shown in Figure 5H (Figure 5I). When the cells were first incubated with MG132 for 1 hour, followed by 1 hour incubation with MV151, in-gel readout proved negative (Figure 5G, lane 3) and the fluorescence in the cells had dramatically decreased (Figure 5J). This competition study proves that the vast majority of the fluorescence observed in cells, after fixation, is due to proteasome labeling.

The results obtained in cell lines raised the question whether MV151 could be used

to label proteasomes in mice. To test the bioavailability of MV151, C57Bl/6 mice were given a single intraperitoneal injection with MV151 (20 $\mu\text{mol/kg}$ body weight) and were sacrificed 24 hours post-injection. Fluorescence microscopic analysis of mouse tissues revealed the capacity of MV151 to penetrate tissues *in vivo*. The highest BODIPY TMR fluorescence was detected in the liver (Figure 6A) and in the pancreas (Figure 6B). Interestingly, BODIPY TMR fluorescence was higher in the peripheries of the tissues, indicating that the probe might reach the liver most efficiently by diffusion from the peritoneal cavity rather than being distributed by entering the bloodstream. A recently developed transgenic mouse model for monitoring the ubiquitin-proteasome system, which is based on the ubiquitous expression of the Ub^{G76V}-GFP reporter¹⁹ was employed to examine the effect of administration of the proteasome probe. It was previously shown that administration of the proteasome inhibitors epoxomicin and MG262 (ZL₃-boronic acid)²⁰ results in a substantial accumulation

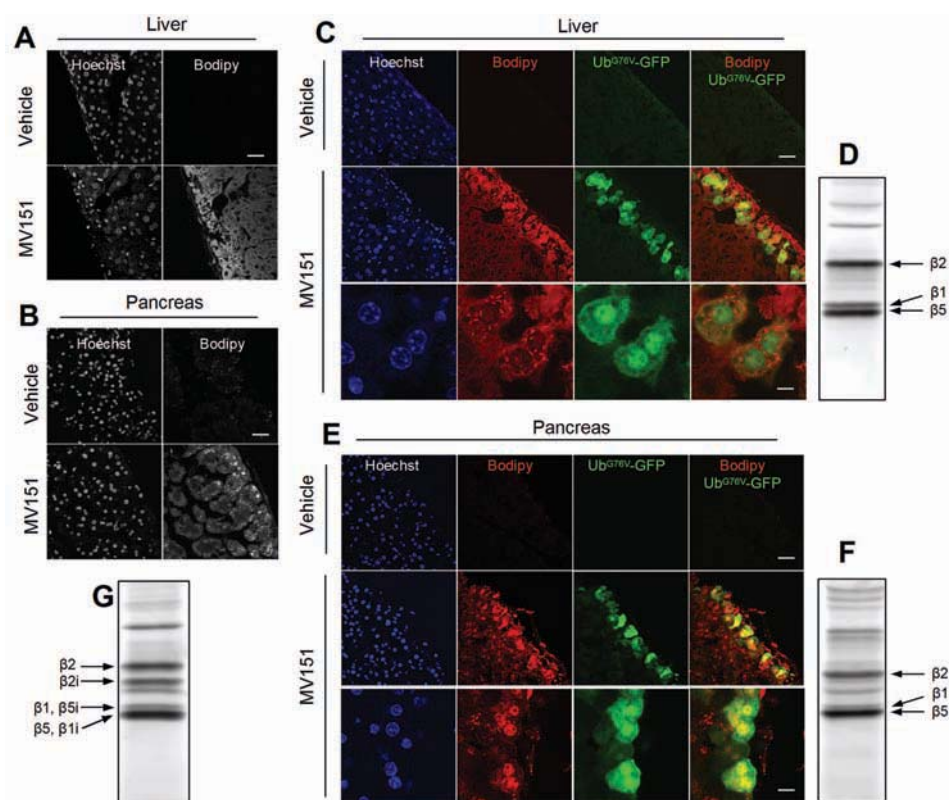


Figure 6. Functional proteasome inhibition in mice.

(A-B) Micrographs of (A) liver and (B) pancreas cryosections from C57Bl/6 mice that were treated with vehicle only or with MV151 (20 $\mu\text{mol/kg}$ body weight). Hoechst staining and BODIPY TMR fluorescence are shown. Scale bar represents 40 μm . (C-F) Micrographs and in-gel fluorescence readout of (C, D) liver and (E, F) pancreas. (C and E) cryosections from Ub^{G76V}-GFP mice that were treated with vehicle only or with MV151 (20 $\mu\text{mol/Kg}$ body weight). Hoechst staining, BODIPY TMR fluorescence, Ub^{G76V}-GFP fluorescence and BODIPY TMR and Ub^{G76V}-GFP merged images are shown. Scale bar represents 40 μm (upper and middle panels) and 5 μm (lower panels). (D-G) SDS-PAGE analysis and in-gel fluorescence readout of homogenates (10 μg total protein) from (D) liver and (F) pancreas tissues (shown in panels C and E) and (G) spleen.

of the Ub^{G76V}-GFP reporter in affected tissues.¹⁹ The accumulation was primarily found in the liver and at higher inhibitor concentrations in other tissues. In the present experiment, the Ub^{G76V}-GFP reporter mice were given a single intraperitoneal injection with MV151 (20 $\mu\text{mol/kg}$ body weight). A total of 24 hours post-injection, the mice were sacrificed and several tissues were analyzed by fluorescence microscopy. Cells accumulating Ub^{G76V}-GFP were detected in the liver (Figure 6C) and the pancreas (Figure 6E), which also contained the highest BODIPY TMR fluorescence of all of the examined tissues (spleen, intestine, kidney, liver, and pancreas). Importantly, all of the cells that accumulated the Ub^{G76V}-GFP reporter contained very high BODIPY TMR fluorescence. The proteasome probe was distributed both in the cytoplasm and nuclei of the cells that accumulated the reporter. Similar to the observations from experiments in cell culture, the affected cells in the mice contained granular accumulations of MV151 in the cytoplasm in close proximity to the nucleus. To verify that accumulation of Ub^{G76V}-GFP in the liver and pancreas coincided with proteasome labeling by MV151, tissue homogenates were analyzed by SDS-PAGE followed by in-gel fluorescence readout. Liver (Figure 6D) and pancreas (Figure 6F) homogenates of animals treated with MV151 revealed that the proteasome catalytic subunits were labeled as expected, although higher background labeling compared to *in vitro* studies was observed. (For Figures 6D and 6F, respectively, the tissues from the images in Figures 6C and 6E were used). SDS-PAGE followed by in-gel fluorescence analysis of spleen homogenates showed labeling of both constitutive and inducible proteasome catalytic subunits (Figure 6G).

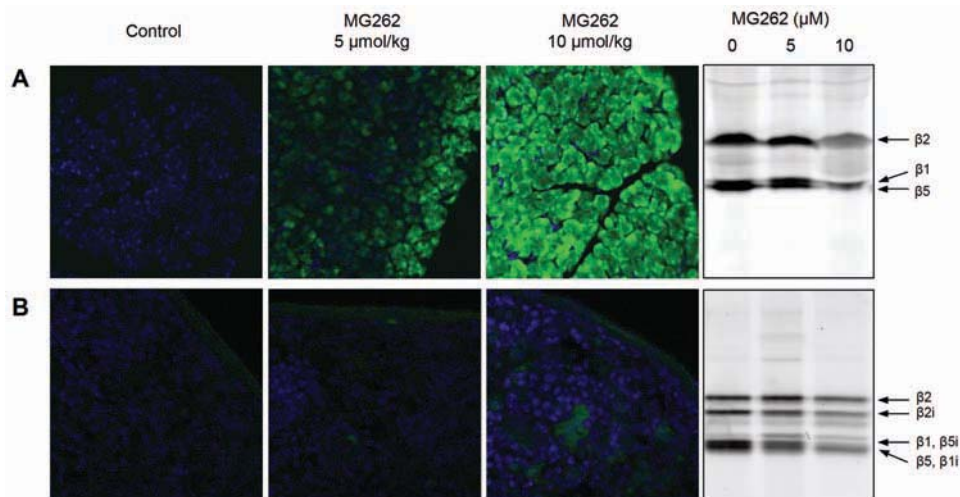


Figure 7. MG262 biodistribution study in Ub^{G76V}-GFP reporter mice.

(A and B) Ub^{G76V}-GFP reporter mice were treated with 0, 5 or 10 $\mu\text{mol/kg}$ bodyweight MG262 by subcutaneous injection and sacrificed after 24 hr. (A) Pancreas and (B) spleen were analyzed. Cryosections of fixed (A) pancreas and (B) spleen were analyzed for accumulation of the reporter by confocal microscopy. GFP in green, Hoechst nuclear stain in blue. Remaining proteasome activity in the (A) pancreas and (B) spleen tissue homogenates was fluorescently labeled by incubation with 0.1 μM MV151 for 1 hr. at 37 $^{\circ}\text{C}$.

As the final set of experiments, the biodistribution of MG262 in Ub^{G76V}-GFP transgenic mice was monitored. The boronic acid MG262 was selected for this purpose because it is both commercially available and most closely resembles the drug bortezomib. Animals were injected subcutaneously with either 5 $\mu\text{mol/kg}$, or 10 $\mu\text{mol/kg}$ body weight of the boronic acid MG262 and were sacrificed 24 hours post-injection. Fluorescence microscopic analysis of spleen and pancreas tissues (Figure 7A and 7B, respectively) showed the concentration-dependent inhibition of the proteasome in MG262-treated Ub^{G76V}-GFP mice, as indicated by increased levels of Ub^{G76V}-GFP reporter. The same tissues were lysed and treated with MV151. SDS-PAGE analysis revealed significant reduction of labeled bands corresponding to the proteasome catalytic subunits when compared with tissue lysates from untreated animals (Figure 7A, pancreas and Figure 7B, spleen).

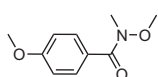
2.3 Conclusion

In summary, the synthesis of MV151 (**3**) as a new fluorescent, cell-permeable proteasome probe is described. MV151 enables broad-spectrum proteasome profiling, both in cell lysates and in living cells. The BODIPY TMR dye proved to be very useful for in-gel readout of labeled active subunits in that it provided a straightforward method for direct and sensitive proteasome profiling and omitted the need for western blotting, radioactivity, and gel drying. MV151 could be readily detected upon administration to mice and correlated with inhibition of the proteasome in the affected tissues. Finally, MV151-mediated proteasome labeling in combination with Ub^{G76V}-GFP transgenic mice is a useful strategy for monitoring the biodistribution of proteasome inhibitors.

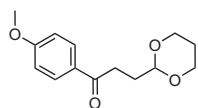
Experimental section

General: All reagents were commercial grade and were used as received unless indicated otherwise. Toluene (Tol.) (purum), ethyl acetate (EtOAc) (puriss.) and light petroleum ether (PetEt) (puriss.) were obtained from Riedel-de Haën and distilled prior to use. Dichloroethane (DCE), dichloromethane (DCM), dimethyl formamide (DMF) and dioxane (Biosolve) were stored on 4Å molecular sieves. Tetrahydrofuran (THF) (Biosolve) was distilled from LiAlH₄ prior to use. Reactions were monitored by TLC-analysis using DC-alufolien (Merck, Kieselgel60, F254) with detection by UV-absorption (254 nm), spraying with 20% H₂SO₄ in ethanol followed by charring at ~150 °C, by spraying with a solution of (NH₄)₆Mo₇O₂₄·4H₂O (25 g/L) and (NH₄)₄Ce(SO₄)₄·2H₂O (10 g/L) in 10% sulfuric acid followed by charring at ~150°C or spraying with an aqueous solution of KMnO₄ (20%) and K₂CO₃ (10%). Column chromatography was performed on Merck silicagel (0.040 – 0.063 nm). Electrospray Ionization Mass spectra (MS (ESI)) were recorded on a PE/Sciex API 165 instrument interface and HRMS (SIM mode) were recorded on a TSQ Quantum (Thermo Finnigan) fitted with an accurate mass option, interpolating between PEG-calibration peaks. ¹H- and ¹³C-APT-NMR spectra were recorded on a Jeol JNM-FX-200 (200/50), a Bruker AV-400 (400/100 MHz) equipped with a pulsed field gradient accessory or a Bruker AV-500 (500/125 MHz). Chemical shifts are given in ppm (δ) relative to tetramethylsilane as internal standard. Coupling constants are given in Hz. All presented ¹³C-APT spectra are proton decoupled. Optical

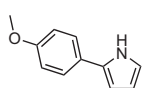
rotations were measured on a Propol automatic polarimeter (Sodium D line, $\lambda = 589$ nm) and ATR-IR spectra were recorded on a Shimadzu FTIR-8300 fitted with a single bounce DurasamplIR diamond crystal ATR-element. UV spectra were recorded on a Perkin Elmer, Lambda 800 UV/VIS spectrometer. Carboxyaldehyde pyrrole (**8**),¹¹ epoxomicin,²¹ dansylAhx₃L₃VS,⁷ NIP-LVS,¹² Z-LVS,¹² AdaAhx₃L₃VS⁶ and Boc-L₃VS¹² were synthesized as described in literature.



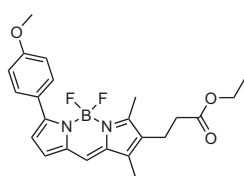
Anisoyl-*N,O*-di-methyl-hydroxamide (5). Anisic acid (**4**) (4.56 g, 30 mmol) was dissolved in DCM before being treated with HCTU (13.65 g, 33 mmol, 1.1 equiv.), *N,O*-dimethylhydroxylamine·HCl (2.93 g, 30 mmol, 1 equiv.) and DiPEA (9.92 ml, 60 mmol, 2 equiv.). The reaction mixture was stirred for 12 hr. before being washed with 1 M HCl (3×) and sat. aq. NaHCO₃ (2×). The DCM layer was separated and dried over MgSO₄ and concentrated. Purification by column chromatography (Tol. → 40% EtOAc in Tol.) gave 5.22 g (26.7 mmol, 89%) of the title compound. ¹H NMR (200 MHz, CDCl₃): δ ppm 7.72 (d, $J = 9.1$ Hz, 2H), 6.90 (d, $J = 9.1$ Hz, 2H), 3.83 (s, 3H), 3.55 (s, 3H), 3.35 (s, 3H). ¹³C NMR (50 MHz, CDCl₃): δ ppm 168.41, 160.89, 129.81, 125.53, 112.52, 59.79, 54.33, 32.77. HRMS: calcd. for [C₁₀H₁₃NO₃H]⁺ 196.09682, found 196.09678.



3-[1,3]Dioxan-2-yl-1-(4-methoxy-phenyl)-propan-1-one (6). Anisoyl-*N,O*-di-methyl-hydroxamide (**5**) (4.7 g, 24 mmol) was dissolved in freshly distilled THF, put under an argon atmosphere and cooled to 0 °C. (1,3-Dioxane-2-ylethyl)-magnesium bromide (72 ml 0.5M in THF, 36 mmol, 1.5 equiv.) was added dropwise over 1 hr. After 3 hr. the reaction mixture was quenched with sat. aq. NH₄Cl and extracted with EtOAc. The organic layer was separated, dried over Na₂SO₄ and concentrated. Column chromatography (Tol. → 20% EtOAc in Tol.) yielded **6** (5.35 g, 21.4 mmol, 89%). ¹H NMR (200 MHz, CDCl₃): δ ppm 7.96 (d, $J = 9.1$ Hz, 2H), 6.93 (d, $J = 8.8$ Hz, 2H), 4.66 (t, $J = 5.1$ Hz, 1H), 4.10 (dd, $J_1 = 4.75$, $J_2 = 10.6$ Hz, 2H), 3.87 (s, 3H), 3.78 (dt, $J_1 = 2.56$, $J_2 = 12.23$ Hz, 2H), 3.06 (t, $J = 7.31$ Hz, 2H), 2.06 (m, 3H), 1.33 (d, $J = 13.16$ Hz, 1H). ¹³C NMR (50 MHz, CDCl₃): δ ppm 197.79, 163.06, 129.98, 129.74, 113.33, 100.84, 66.51, 55.11, 31.97, 29.24, 25.48. HRMS: calcd. for [C₁₄H₁₈O₄H]⁺ 251.12779, found 251.12768.

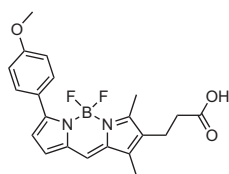


2-(4-Methoxy-phenyl)-1H-pyrrole (7). Ketone **6** (5.1 g, 20.4 mmol) was coevaporated with Tol. (2×), dissolved in glacial acetic acid (100 ml) and put under an argon atmosphere, before NH₄OAc (18.8 g, 244.8 mmol, 12 equiv.) and Ac₂O (7.14 ml, 75.5 mmol, 3.7 equiv.) were added. The reaction mixture was refluxed for 3 hr., poured into H₂O, neutralized with sat. aq. NaHCO₃ and extracted with DCM. The DCM layer was separated, dried over Na₂SO₄ and concentrated. Purification by column chromatography (PetEt → 10% EtOAc in PetEt) gained the title compound **7** (2.46 g, 14.2 mmol, 70%). ¹H NMR (200 MHz, CDCl₃): δ ppm 9.33 (s, 1H), 7.41 (2H), 6.87 (2H), 6.77 (1H), 6.40 (m, 1H), 6.24 (1H), 3.78 (s, 3H). ¹³C NMR (50 MHz, CDCl₃): δ ppm 157.73, 131.89, 125.98, 124.94, 118.21, 114.03, 109.18, 104.26, 55.04.



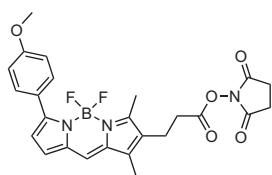
4,4-Difluoro-1,3-dimethyl-2-(2-(ethoxycarbonyl)ethyl)-7-(4-methoxy-phenyl)-4-bora-3a,4a-diaza-s-indacene (9). Methoxyphenyl pyrrole **7** (5.79 g, 33 mmol, 1 equiv.) and carboxyaldehyde pyrrole **8**¹¹ (7.47 g, 33 mmol, 1 equiv.) were dissolved in EtOH (40 ml). The resulting mixture was cooled to 0 °C, and HBr (5.5 ml 48% solution in water, 50 mmol, 1.5 equiv.) was added. After 1hr. stirring, TLC analysis showed complete consumption of the starting materials. The purple precipitate was collected by filtration. The crude dipyrrole HBr salt was coevaporated with DCE and dissolved in DCE (750 ml) under argon atmosphere. TEA (7.74 ml, 55.5 mmol, 3 equiv.) and BF₃·Et₂O (11.7 ml, 92.5 mmol, 5 equiv.) were added, and the reaction was subsequently refluxed at 90 °C. After 30 min., the solution was cooled to room temperature, filtered over a plug of basic alumina and concentrated. Silica gel column chromatography (Tol. → 2.5% EtOAc in Tol.) gave

the title compound **9** (5.37 g, 12.6 mmol, 68%). $^1\text{H NMR}$ (200 MHz, CDCl_3): δ ppm 7.87 (d, $J = 8.8\text{ Hz}$, 2H), 7.06 (s, 1H), 6.96 (d, $J = 8.8\text{ Hz}$, 2H), 6.92 (d, $J = 5.8\text{ Hz}$, 1H), 6.52 (d, $J = 4.4\text{ Hz}$, 1H), 4.11 (q, $J = 7.3\text{ Hz}$, 2H), 3.84 (s, 3H), 2.71 (t, $J = 7.1\text{ Hz}$, 2H), 2.53 (s, 3H), 2.42 (t, $J = 7.3\text{ Hz}$, 2H), 2.18 (s, 3H), 1.23 (t, $J = 7.3\text{ Hz}$, 3H). $^{13}\text{C NMR}$ (50 MHz, CDCl_3): δ ppm 172.13, 160.09, 158.64, 155.15, 139.53, 134.80, 133.95, 130.40, 129.67, 127.76, 125.16, 122.67, 117.91, 113.42, 60.23, 54.86, 33.67, 19.08, 13.86, 12.77, 9.10. HRMS: calcd. for $[\text{C}_{23}\text{H}_{25}\text{BF}_2\text{N}_2\text{O}_3\text{H}]^+$ 427.19991, found 427.20030.



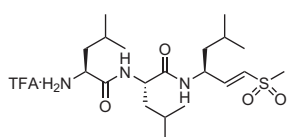
4,4-Difluoro-1,3-dimethyl-2-(2-carboxyethyl)-7-(4-methoxy-phenyl)-4-bora-3a,4a-diaza-s-indacene (10).

Ethyl ester **9** (44 mg, 0.1 mmol) was dissolved in dioxane (2 ml). After addition of 0.1M aq. NaOH (1mL, 0.1 mmol, 1 equiv.) and stirring overnight, the purple suspension was diluted with EtOAc, extracted with 1M HCl, dried over MgSO_4 and concentrated. Column chromatography (Tol. \rightarrow 1% EtOAc and 1% AcOH in Tol.) yielded BODIPY acid **10** (15 mg, 40 μmol , 40%). $^1\text{H NMR}$ (200 MHz, CDCl_3): δ ppm 7.87 (d, $J = 8.8\text{ Hz}$, 2H), 7.03 (s, 1H), 6.95 (d, $J = 8.8\text{ Hz}$, 2H), 6.89 (d, $J = 4.4\text{ Hz}$, 1H), 6.50 (d, $J = 3.7\text{ Hz}$, 1H), 6.24 (1H), 3.81 (s, 3H), 2.68 (t, $J = 7.3\text{ Hz}$, 2H), 2.51 (s, 3H), 2.45 (t, $J = 7.3\text{ Hz}$, 2H), 2.21 (s, 3H). $^{13}\text{C NMR}$ (50 MHz, CDCl_3): δ ppm 178.44, 160.33, 158.76, 155.75, 139.62, 135.04, 134.13, 130.65, 129.40, 128.13, 125.40, 122.91, 118.30, 113.66, 55.17, 33.76, 19.11, 12.98, 9.41. HRMS: calcd. for $[\text{C}_{21}\text{H}_{21}\text{BF}_2\text{N}_2\text{O}_3\text{H}]^+$ 399.16861, found 399.16904, calcd. for $[\text{C}_{21}\text{H}_{21}\text{BF}_2\text{N}_2\text{O}_3\text{Na}]^+$ 421.15055, found 421.15096.

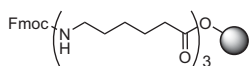


BODIPY TMR-OSu (11).

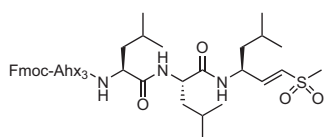
BODIPY TMR-OH (**10**, 28 mg, 70 μmol) was coevaporated thrice with Tol., before being dissolved in DCM (1 ml). After the addition of HOSu (32 mg, 0.28 mmol, 4 equiv.) and EDC-HCl (54 mg, 0.28 mmol, 4 equiv.), the reaction mixture was stirred overnight. Next, the reaction was diluted with EtOAc, washed with 1M aq. HCl, dried over MgSO_4 and concentrated. Purification by column chromatography (Tol. \rightarrow 5% EtOAc in Tol.) furnished title compound **11** (24 mg, 48 μmol , 69%). $^1\text{H NMR}$ (200 MHz, CDCl_3): δ ppm 7.88 (d, $J = 8.8\text{ Hz}$, 2H), 7.10 (s, 1H), 6.97 (m, 3H), 6.55 (d, $J = 4.4\text{ Hz}$, 1H), 3.85 (s, 3H, Me), 2.79 (m, 8H), 2.54 (s, 3H), 2.20 (s, 3H). $^{13}\text{C NMR}$ (50 MHz, CDCl_3): δ ppm 168.92, 167.58, 160.49, 158.21, 156.30, 139.62, 135.22, 133.98, 130.74, 128.46, 128.28, 125.31, 123.15, 118.61, 113.72, 55.23, 30.85, 25.51, 19.11, 13.01, 9.56. HRMS: calcd. for $[\text{C}_{25}\text{H}_{24}\text{BF}_2\text{N}_3\text{O}_5\text{H}]^+$ 496.18498, found 496.18453, calcd. for $[\text{C}_{25}\text{H}_{24}\text{BF}_2\text{N}_3\text{O}_5\text{NH}_4]^+$ 513.21153, found 513.21151, calcd. for $[\text{C}_{25}\text{H}_{24}\text{BF}_2\text{N}_3\text{O}_5\text{Na}]^+$ 518.16693, found 518.16706.



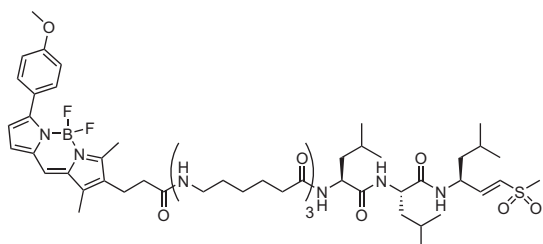
TFA-L₃VS (13). Boc-L₃VS¹² (**12**) (0.47 g, 0.9 mmol) was dissolved in a mixture of TFA/DCM (1/1) and was stirred for 30 min. The reaction mixture was concentrated *in vacuo* affording the TFA salt **13** as a white solid which was used without further purification.



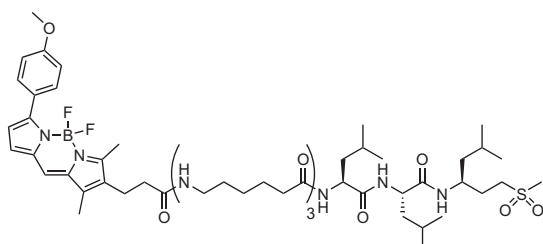
Fmoc-Ahx₃-Wang (14). Wang resin (1.8 g, 1.1 mmol/g, 2 mmol) was coevaporated with DCE (2 \times) and condensed with Fmoc-Ahx-OH (2.1 g, 6 mmol, 3 equiv.) under the influence of DIC (1.0 ml, 6.6 mmol, 3.3 equiv.) and DMAP (12 mg, 0.1 mmol, 0.05 equiv.) for 2hr. The resin was then filtered and washed with DCM (3 \times) and subjected to a second condensation sequence. The loading of the resin was determined to be 0.8 mmol/g (2.30 g, 1.84 mmol, 92%) by spectrophotometric analysis. The obtained resin was submitted to two cycles of Fmoc solid-phase synthesis with Fmoc-Ahx-OH, as follows: a) deprotection with piperidine/NMP (1/4, v/v, 15 min.); b) wash with NMP (3 \times); c) coupling of Fmoc-Ahx-OH (1.63 g, 4.6 mmol, 2.5 equiv.) in the presence of BOP (2.0 g, 4.6 mmol, 2.5 equiv.) and DiPEA (0.91 ml, 5.5 mmol, 3 equiv.) in NMP and shake for 2hr.; d) wash with NMP (3 \times) and DCM (3 \times). Couplings were monitored for completion by the Kaiser test.²²



Fmoc-Ahx₃L₃VS (15). The tripeptide Fmoc-Ahx₃-OH was released from resin **14** (0.45 mmol) by treatment with TFA/DCM (1/1, v/v, 30 min., 3×). The fractions were collected and coevaporated with Tol. (3×). The crude Fmoc-Ahx₃-OH was dissolved in DCM/DMF (99/1, v/v) and condensed with the crude TFA·L₃VS (**13**, 0.9 mmol, 2 equiv.) under the influence of BOP (0.49 g, 1.13 mmol, 2.5 equiv.) and DiPEA (0.45 ml, 2.7 mmol, 6 equiv.). The reaction mixture was stirred overnight, before being concentrated *in vacuo*. The residue was dissolved in chloroform and washed with 1M HCl and sat. aq. NaHCO₃. The organic layer was dried over MgSO₄ and concentrated. Silica column chromatography (DCM → 4% MeOH in DCM) yielded the title compound **15** (0.41 g, 0.44 mmol, 98%). ¹H NMR (500 MHz, CDCl₃/MeOD): δ ppm 7.77 (d, *J* = 7.5 Hz, 2H), 7.61 (d, *J* = 7.5 Hz, 2H), 7.40 (t, *J* = 7.5 Hz, 2H), 7.31 (t, *J* = 7.5 Hz, 2H), 6.82 (dd, *J*₁ = 15, *J*₂ = 5.0 Hz, 1H), 6.52 (d, *J* = 15 Hz, 1H), 4.68 (m, 1H), 4.36 (m, 4H), 4.21 (t, *J* = 6.8 Hz, 1H), 3.16 (m, 6H), 2.93 (s, 3H), 2.26-2.14 (m, 6H), 1.62-1.40 (m, 21H), 0.95-0.89 (m, 18H). ¹³C NMR (125 MHz, CDCl₃): δ ppm 174.15, 173.95, 173.87, 173.04, 172.96, 171.98, 171.90, 156.82, 156.78, 147.50, 143.66, 141.00, 128.84, 127.42, 124.74, 124.58, 119.67, 66.25, 51.82, 51.75, 47.62, 47.52, 46.95, 42.35, 42.15, 40.41, 40.28, 39.95, 38.88, 38.75, 35.92, 35.81, 35.49, 29.09, 28.59, 26.02, 25.94, 25.88, 25.06, 24.96, 24.84, 24.54, 24.50, 25.44, 22.52, 22.50, 22.48, 21.46, 21.36. HRMS: calcd. for [C₅₃H₈₂N₆O₉SH]⁺ 979.59368, found 979.59276.



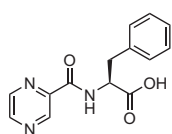
BODIPY TMR-Ahx₃L₃VS (3). DBU (30 μl, 0.2 mmol, 1 equiv.) was added to a solution of **15** (0.2 g, 0.2 mmol) in DMF. After 5 min. of stirring, HOBT (0.12 g, 0.9 mmol, 4.5 equiv.) was added. To this mixture, BODIPY TMR-OSu (**11**, 0.1 g, 0.2 mmol, 1 equiv.) and DiPEA (0.2 ml, 1.2 mmol, 6 equiv.) were added, and the mixture was stirred for 30 min., before being concentrated *in vacuo*. Purification by column chromatography (0.1% TEA in DCM → 3% MeOH and 0.1% TEA in DCM) afforded BODIPY TMR-Ahx₃L₃VS (**3**) (0.22 g, 197 μmol, 99%). ¹H NMR (500 MHz, CDCl₃): δ ppm 7.87 (d, *J* = 8.5 Hz, 2H), 7.52 (s, 1H), 7.51 (s, 1H), 7.35 (d, *J* = 8 Hz, 1H), 6.97 (m, 5H), 6.81 (dd, *J*₁ = 15, *J*₂ = 5 Hz, 1H), 6.79 (s, 1H), 6.55 (d, *J* = 4 Hz, 1H), 6.51 (d, *J* = 15 Hz, 1H), 4.67 (m, 1H), 4.33 (m, 2H), 3.86 (s, 3H), 3.17 – 3.10 (m, 6H), 2.96 (s, 3H), 2.74 (t, *J* = 7.3 Hz, 2H), 2.53 (s, 3H), 2.30 (t, *J* = 7.3 Hz, 2H), 2.21 (m, 5H), 2.14 (t, *J* = 7.3 Hz, 2H), 2.08 (t, *J* = 7.3 Hz, 2H), 1.66-1.17 (m, 27H), 0.95-0.89 (m, 18H). ¹³C NMR (125 MHz, CDCl₃): δ ppm 174.40, 174.01, 173.94, 173.20, 172.53, 172.45, 172.06, 160.16, 159.44, 155.16, 147.61, 140.04, 134.77, 134.23, 130.46, 128.87, 128.30, 127.81, 125.29, 122.72, 118.10, 113.55, 55.12, 52.11, 52.04, 47.72, 45.98, 42.46, 42.26, 40.33, 40.00, 39.08, 38.94, 38.80, 35.93, 35.74, 35.62, 28.63, 28.49, 26.04, 25.99, 25.86, 25.03, 24.96, 24.88, 24.63, 24.60, 24.55, 22.66, 22.62, 22.58, 21.54, 21.48, 21.43, 20.09, 12.84, 9.27, 8.36. HRMS: calcd. for [C₅₉H₉₁BF₂N₈O₉SH]⁺ 1137.67636, found 1137.67442, for [C₅₉H₉₁BF₂N₈O₉SNH₄]⁺ 1154.70291, found 1154.70149, for [C₅₉H₉₁BF₂N₈O₉SNa]⁺ 1159.65831, found 1159.65690. [α]_D²³ = -44 (c 0.1, MeOH). λ_{max} (MeOH): 544.43 nm, ε: 60400 l mol⁻¹ cm⁻¹.



BODIPY TMR-Ahx₃L₃ES (16). A catalytic amount of 10% Pd/C was added to a solution of **15** (49 mg, 50 μmol) in MeOH. Hydrogen gas was bubbled through the solution for 2 hr., after which the catalyst was filtered off and the reaction mixture was concentrated *in vacuo*. The residue was dissolved in DMF and treated with DBU (7.5 μL, 50 μmol, 1 equiv.) for 5 min., before HOBT (30 mg, 0.23 mmol, 4.5 equiv.) was added. To this mixture, BODIPY TMR-OSu (**11**, 25 mg, 50 μmol, 1 equiv.) and DiPEA (50

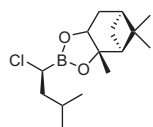
μL , 0.3 mol, 6 equiv.) were added, and the mixture was stirred for 30 min., before being concentrated *in vacuo*. Purification by column chromatography (0.1% TEA in DCM \rightarrow 3% MeOH and 0.1% TEA in DCM) yielded BODIPY TMR-Ahx₃L₃ES (**16**, 50.3 mg, 44 μmol , 88 %). ¹H NMR (500 MHz, CDCl₃/MeOD): δ ppm 7.78 (d, J = 8.5 Hz, 2H), 7.41 (m, 1H), 7.18 (m, 1H), 7.08 (m, 3H), 6.80 (m, 3H), 6.47 (d, J = 4.0 Hz, 1H), 4.18 (m, 2H), 3.92 (m, 1H), 3.78 (s, 3H), 3.07-2.99 (m, 6H), 2.87 (s, 3H), 2.65 (t, J = 7.5 Hz, 2H), 2.44 (s, 3H), 2.22 (t, J = 7.5 Hz, 2H), 2.14 (m, 5H), 2.06 (t, J = 7.3 Hz, 2H), 1.99 (t, J = 7.5 Hz, 2H), 1.95 (m, 1H), 1.77 (m, 1H), 1.56-1.11 (m, 27H), 0.88-0.78 (m, 18H). ¹³C NMR (125 MHz, CDCl₃): δ ppm 174.57, 174.05, 173.14, 172.56, 172.39, 172.31, 160.10, 159.38, 155.08, 140.01, 134.72, 134.18, 130.39, 128.76, 127.96, 127.76, 125.23, 122.70, 117.34, 55.03, 52.26, 52.15, 51.28, 46.03, 45.95, 43.64, 40.17, 40.11, 39.90, 38.91, 38.78, 35.83, 35.77, 35.68, 35.45, 28.56, 28.41, 27.87, 26.02, 25.96, 25.84, 25.02, 24.96, 24.83, 24.63, 24.57, 24.53, 22.72, 22.52, 21.51, 21.37, 21.23. HRMS: calcd. for [C₅₉H₉₃BF₂N₈O₉SH]⁺ 1139.69201, found 1139.69203.

Synthesis of dipeptidyl pinanediol boronic ester (Figure 4, entry C).



3-Phenyl-2-[(pyrazine-2-carbonyl)-amino]-propionic acid (Pyr-Phe-OH). Oxalylchloride (6.0 ml, 70 mmol, 1.9 equiv.) and 6 drops of DMF were added to a suspension of pyrazinecarboxylic acid HCl salt (5.26 g, 42.2 mmol, 1.7 equiv.) in Et₂O at 0 °C and stirred for 2 days, before being concentrated. The resulting purple residue was resuspended in Et₂O

and cooled to 0 °C, before L-phenylalanine methyl ester (7.95 g, 36.8 mmol) was added. TEA (25 ml, 179 mmol, 4.9 equiv.) was added dropwise over 10 min. The reaction mixture was stirred for 12 hr. before being poured into H₂O and extracted with EtOAc (3 \times 100 ml). The combined organic layers were dried over MgSO₄ and concentrated, giving a red oil. Purification by column chromatography (50% EtOAc in PetEt) gave 8.93 g (31.2 mmol, 85%) Pyr-Phe-OMe. ¹H NMR (200 MHz, CDCl₃): δ ppm 9.37 (s, 1H), 8.75 (d, J = 2.2 Hz, 2H), 8.52 (d, J = 2.2 Hz, 1H), 8.22 (d, J = 8.0 Hz, 1H), 7.22 (m, 5H), 5.08 (m, 1H), 3.75 (s, 3H), 3.27 (m, 2H). ¹³C NMR (50 MHz, CDCl₃): δ ppm 170.8, 162.0, 146.8, 143.5, 143.2, 142.1, 135.4, 128.5, 127.8, 126.3, 52.7, 51.6, 37.1. [α]_D²³ = +64.3 (c 1.25, DCM). To a solution of Pyr-Phe-OMe (8.40 g, 29.5 mmol) in dioxane/MeOH (5/2, v/v), NaOH (9.5 ml 4M in H₂O, 38 mmol, 1.3 equiv.) was added and the reaction mixture was stirred for 2 hr. 1M NaHSO₄ (36 ml) was added and the mixture was concentrated *in vacuo*. The residue was taken up in EtOAc, washed with brine, dried over MgSO₄ and concentrated to yield Pyr-Phe-OH as a white solid (7.88 g, 29.2 mmol, 99%). ¹H NMR (200 MHz, CDCl₃): δ ppm 9.40 (s, 1H), 9.37 (s, 1H), 8.76 (s, 1H), 8.54 (s, 1H), 8.21 (d, J = 8.0 Hz, 1H), 7.25 (m, 5H), 5.13 (m, 1H), 3.31 (m, 2H). ¹³C NMR (50 MHz, CDCl₃): δ ppm 174.0, 164.7, 148.7, 145.6, 144.7, 144.6, 137.9, 130.3, 129.5, 127.9, 54.9, 38.2. MS (ESI): m/z 272.0 [M+H]⁺. [α]_D²³ = +29.4 (c 1.0, EtOH).

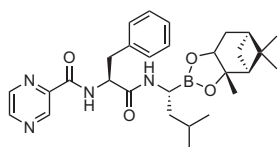


(1R)-4-(1-chloro-3-methylbutyl)-2,9,9-trimethyl-3,5-dioxo-4-bora-

tricyclo[6.1.1.0^{2,6}]decane. (2-methyl)-propylboronic acid (2.22 g, 21.8 mmol) was dissolved in THF and (+)-(1S,2S,3R,5S)-pinanediol was added. The reaction mixture was stirred overnight and concentrated *in vacuo*. Purification by column chromatography (3% EtOAc in PetEt) gave

4.54 g (20.3 mmol, 93%) of 4-isobutyl-2,9,9-trimethyl-3,5-dioxo-4-bora-tricyclo[6.1.1.0^{2,6}]decane as a colorless oil. ¹H NMR (200 MHz, CDCl₃): δ ppm 4.25 (dd, J_1 = 8.8, J_2 = 2.2 Hz, 1H), 2.41-2.17 (m, 2H), 2.05 (m, 1H), 1.95-1.79 (m, 3H), 1.38 (s, 3H), 1.29 (s, 3H), 1.14 (d, J = 11 Hz, 1H), 0.94 (d, J = 7.3 Hz, 6H), 0.84 (s, 3H), 0.78 (d, J = 7.3 Hz, 2H). ¹³C NMR (50 MHz, CDCl₃): δ ppm 85.1, 77.4, 51.2, 39.5, 38.0, 35.5, 28.7, 27.0, 26.5, 25.2, 24.8, 24.0. [α]_D²³ = 28.4 (c 1.0, DCM). *n*BuLi (7.0 ml 1.6M in hexane, 11.2 mmol, 1.12 equiv.) was added to a solution of DCM (0.90 ml, 14.0 mmol, 1.4 equiv.) in THF (40 ml) at -80 °C and stirred for 1 hr. To the stirred reaction mixture a solution of 4-isobutyl-2,9,9-trimethyl-3,5-dioxo-4-bora-tricyclo[6.1.1.0^{2,6}]decane (2.36 g, 10.0 mmol) in THF (40 ml) was added and stirred for 1 hr. at -80 °C before a solution of ZnCl₂ (20 ml 1M in diethyl ether, 20 mmol, 10 equiv.) was added dropwise over 10 min. The reaction mixture was allowed to warm up to -40 °C in 2 hr., before it was allowed to warm up to room temperature and stirred for 2 hr. The resulting

reaction mixture was poured into 250 ml H₂O and extracted with EtOAc (3 × 100 ml). The combined organic layers were dried over MgSO₄ and concentrated. Purification by column chromatography (2% EtOAc in PetEt) gave the title compound as a colorless oil (2.68 g, 0.94 mmol, 94%). ¹H NMR (200 MHz, CDCl₃): δ ppm 4.36 (dd, *J*₁ = 9.1, *J*₂ = 1.8 Hz, 1H), 3.54 (dd, *J* = 9.9, *J* = 5.9 Hz, 1H), 2.44-2.18 (m, 2H), 2.09 (m, 1H), 1.99-1.73 (m, 4H), 1.68-1.55 (m, 1H), 1.42 (s, 1H), 1.30 (s, 1H), 1.19 (d, *J* = 10.9 Hz, 1H), 0.92 (m, 6H), 0.85 (s, 3H). ¹³C NMR (50 MHz, CDCl₃): δ ppm 86.2, 78.1, 50.9, 42.5, 39.1, 37.9, 35.0, 28.2, 26.8, 26.0, 25.3, 23.7, 22.7, 21.0. [α]_D²³ = +44.2 (c 1.0, DCM).



Pyrazine-2-carboxylic acid (1-[3-methyl-1-(2,9,9-trimethyl-3,5-dioxa-4-bora-tricyclo[6.1.1.0^{2,6}]dec-4-yl)-butylcarbamoyl]-2-phenyl-ethyl)-amide.

DIC (175 μl, 1.13 mmol, 1.3 equiv.) was added to a solution of Pyr-Phe-OH (239 mg, 0.88 mmol) and HOSu (129 mg, 1.12 mmol) in DCM (10 ml) and the reaction mixture was stirred for 12 hr., yielding the crude Pyr-Phe-OSu solution. Lithium bis(trimethylsilyl)amide (0.75 ml 1M in THF, 0.75 mmol, 1.3 equiv.) was added to a solution of (1*R*)-4-(1-chloro-3-methyl(butyl)-2,9,9-trimethyl-3,5-dioxa-4-bora-tricyclo[6.1.1.0^{2,6}]decane (165 mg, 0.58 mmol) in THF (6 ml) at -80 °C. The reaction mixture was allowed to warm up to room temperature and was stirred for 12 hr. before it was cooled to -80 °C. HCl (2 ml 2M in diethyl ether) was added and the reaction mixture was allowed to warm to 5 °C, before being cooled to -80 °C. To the stirred solution DiPEA (1.2 ml, 7.3 mmol, 12.6 equiv.) and the crude Pyr-Phe-OSu solution (0.88 mmol, 1.5 equiv.) were added and the reaction mixture was allowed to warm up to room temperature. The reaction mixture was stirred for an additional 2 hr. before being filtered over hyflo and the filtrate was concentrated. Purification of the residue by column chromatography (10% EtOAc in PetEt → 50% EtOAc in PetEt) gave 185 mg (0.36 mmol, 62%) of the title compound. ¹H NMR (400 MHz, MeOD): δ ppm 9.1 (d, *J* = 1.4 Hz, 1H), 8.76 (d, *J* = 2.4 Hz, 1H), 8.64 (d, *J* = 2.4 Hz, 1H), 7.18-7.30 (m, 5H), 5.04 (m, 1H), 4.23 (m, 1H), 3.78 (m, 2H), 3.20 (m, 2H), 2.74 (m, 1H), 2.33 (m, 1H), 2.13 (m, 1H), 1.95 (m, 1H), 1.82 (m, 2H), 1.54 (m, 1H), 1.36 (s, 3H), 1.27 (s, 3H), 1.19 (d, *J* = 11 Hz, 1H), 1.08 (d, *J* = 6.6 Hz, 6H), 0.86 (s, 3H). ¹³C NMR (100 MHz, CDCl₃/MeOD): δ ppm 171.9, 162.4, 146.9, 143.5, 143.3, 142.6, 135.4, 128.9, 127.9, 126.4, 84.1, 76.5, 52.2, 51.2, 40.9, 39.4, 39.2, 38.0, 37.5, 35.4, 28.1, 26.5, 25.8, 24.7, 23.4, 22.6, 21.1. MS (ESI): *m/z* 519.4 [M+H]⁺, 367.1 [M-pinanediol-H₂O+H]⁺.

Proteasomal activity measurement using fluorogenic substrates

Protein lysates from EL-4 (1 mg/ml) were incubated with various concentrations of MV151 (**3**) for 1 hr. at 37°C. For measurement of proteasomal activities, 10 μg of the labeled lysate were added to 100 μl of substrate buffer, containing 20 mM HEPES, pH 8.2, 0.5 mM EDTA, 1% DMSO, 1 mM ATP and 10 μM Z-Ala-Arg-Arg-AMC (trypsin-like), 60 μM Suc-Leu-Leu-Val-Tyr-AMC (chymotrypsin-like) or 60 μM Z-Leu-Leu-Glu-βNA (caspase-like). Fluorescence was measured every min. for 25 min. at 37°C using a Fluostar Optima 96 well plate reader (BMG Labtechnologies) ($\lambda_{\text{ex}}/\lambda_{\text{em}} = 355/450$ nm for AMC and 320/405 nm for βNA) and the maximum increase in fluorescence per min. was used to calculate specific activities of each sample. Nonspecific hydrolysis was assessed by preincubation with 1 μM epoxomicin for 1 hr. at 37°C and was subtracted from each measurement.

In-gel detection of labeled proteasome subunits

Whole cell lysates were made in lysis buffer containing 50 mM Tris pH 7.5, 1 mM DTT, 5 mM MgCl₂, 250 mM sucrose, 2 mM ATP. Protein concentration was determined by the colorimetric Bradford method. For the labeling reactions, 10 μg of total protein lysates were incubated for 1 hr. at 37°C with increasing concentrations of MV151 in a total reaction volume of 10 μl. Where indicated, 50 ng purified 20S proteasome (BioMol) was used. For competition studies, cell lysates (10μg) were exposed to the known inhibitors for 1hr

prior to incubation with MV151 (0.1 μ M) for 1 hr. at 37°C. For assessment of background labeling, heat inactivated lysates (10 μ g, boiled for 3 min with 1% SDS) were treated with MV151. Reaction mixtures were boiled with Laemmli's buffer containing β -mercapto-ethanol for 3 min and resolved on 12.5% SDS-PAGE. In-gel visualization was performed in the wet gel slabs directly using the Cy3/Tamra settings (λ_{ex} 532, λ_{em} 560) on the Typhoon Variable Mode Imager (Amersham Biosciences). Labeling profiles in living cells were determined by incubating approximately $1 \cdot 10^6$ cells with 1 to 10 μ M MV151 in culture medium at 37°C for 8 hr. Cells were lysed followed by in gel detection as described above.

Cell culture

The human cervical epithelial carcinoma cell line HeLa, the human melanoma cell line MeJuSo and the murine lymphoid cell line EL-4 were cultured in RPMI medium (Sigma-Aldrich) supplemented with 10% fetal calf serum (Sigma-Aldrich), 10 units/ml penicillin and 10 μ g/ml streptomycin (Sigma-Aldrich).

Microscopy

Some $5 \cdot 10^5$ cells were seeded on 35 mm petridishes with 14 mm microwell nr 1.5 coverslips, glassbottom microwell dishes (MatTek Corp, Ashland, MA, USA) and allowed to attach overnight. Cells were visualized with a 60 \times oil immersion lens (Nikon) on a Nikon Eclipse TE 2000U microscope equipped with Radiance 2100 MP integrated laser and detection system (BioRad) and a Tsunami Multiphoton laser module (Spectra Physics). LaserSharp 2K (BioRad) software was used for microscope control and data acquisition and Image Pro 3DS 5.1 (Media Cybernetics Inc) software for image processing. GFP was excited at λ_{ex} 488 nm and detected at 500-530 nm. MV151 and MV152 were excited at λ_{ex} 543 nm and detected at 560-620 nm. CLSM images were adjusted for brightness and contrast using Photoshop software.

Mouse experiments

All animal experiments were approved by the Ethical Committee in Stockholm (Ethical permission number N-46/04 and N18/05). Mice were housed according to Swedish animal care protocols with a 12 hr. day/ light cycle, and fed standard laboratory chow and tap water ad libitum. Adult C57Bl/6 and Ub^{G76V}GFP/1 mice,¹⁶ matched for sex and age were given a single intraperitoneal injection of vehicle (60% DMSO, 40% PBS), MV151 (20 μ mol/Kg body weight), or MG262 (Affiniti) (5 or 10 μ mol/kg body weight) in a total volume of 200 μ l. Based on prior experience in our lab, the boronic acid inhibitors proved to be more potent and show better tissue penetration *in vivo* compared to the vinyl sulfone inhibitors. Therefore, the 20 μ mol/kg bodyweight dose was chosen for MV151, which showed no apparent toxicity in mice. Mice were euthanized 24h after injection by anesthetization with inhaled isoflurane (4.4% in oxygen) followed by transcardial perfusion with 50ml PBS for removal of contaminating blood. Tissues collected for immunocytochemical analysis were processed as described previously.¹⁶ Briefly, 12 μ m cryosections were fixed for 15 min. in 4% paraformaldehyde/PBS, washed in PBS, and where mentioned, Hoechst nuclear stain (2 μ g/ml in H₂O), was applied for 15 min. in the dark followed by washing in PBS. Sections were mounted in a matrix containing 2.5% DABCO (Aldrich). Confocal microscopy was performed on a Zeiss LSM 510 META system. Tissues isolated for in gel analysis were lysed with a Heidolph tissue homogenizer in 300 μ l lysis buffer and further treated as described above.

References and notes

1. Rock, K.L.; Goldberg, A.L. *Annu. Rev. Immunol.* **1999**, *17*, 739-779.
2. Baumeister, W.; Walz, J.; Zuhl, F.; Seemuller, E. *Cell* **1998**, *92*, 367-380.
3. Voges, D.; Zwickl, P.; Baumeister, W. *Annu. Rev. Biochem.* **1999**, *68*, 1015-1068.

4. Kisselev, A.F.; Goldberg, A.L. *Chem. Biol.* **2001**, *8*, 739-758.
5. Ovaas, H.; Overkleeft, H.S.; Kessler, B.M.; Ploegh, H.L. Protein Degradation: The Ubiquitin-Proteasome System, Volume 2 (Wiley-VCH), **2006**, 51-78.
6. Kessler, B.M.; Tortorella, D.; Altun, M.; Kisselev, A.F.; Fiebigler, E.; Hekking, B.G.; Ploegh, H.L.; Overkleeft, H.S. *Chem. Biol.* **2001**, *8*, 913-929.
7. Berkers, C.R.; Verdoes, M.; Lichtman, E.; Fiebigler, E.; Kessler, B.M.; Anderson, K.C.; Ploegh, H.L.; Ovaas, H.; Galardy, P.J. *Nat. Methods* **2005**, *2*, 357-362.
8. Kang, H.C., and Haugland, R.P. December 1993. U.S. patent 5,274,113.
9. Kang, H.C., and Haugland, R.P. September 1995. U.S. patent 5,451,663.
10. Haugland, R.P., and Kang, H.C. September 1988. U.S. patent 4,774,339.
11. Boiadjiev, S.E.; Lightner, D.A. *J. Heterocycl. Chem.* **2003**, *40*, 181-185.
12. Bogoy, M.; McMaster, J.S.; Gaczynska, M.; Tortorella, D.; Goldberg, A.L.; Ploegh, H.L. *Proc. Natl. Acad. Sci. USA.* **1997**, *94*, 6629-6634.
13. Kisselev, A.F.; Goldberg, A.L. *Methods Enzymol.* **2005**, *398*, 364-78.
14. Meng, L.; Mohan, R.; Kwok, B.H.; Elofsson, M.; Sin, N.; Crews, C.M. *Proc. Natl. Acad. Sci. USA.* **1999**, *96*, 10403-10408.
15. Hideshima, T.; Richardson, P.; Chauhan, D.; Palombella, V.J.; Elliott, P.J.; Adams, J.; Anderson, K.C. *Cancer Res.* **2001**, *61*, 3071-3076.
16. Dantuma, N.P.; Lindsten, K.; Glas, R.; Jellne, M.; Masucci, M.G. *Nat. Biotechnol.* **2000**, *18*, 538-543.
17. Reits, E.A.; Benham, A.M.; Plougastel, B.; Neefjes, J.J.; Trowsdale, J. *EMBO J.* **1997**, *16*, 6087-6094.
18. Zhu, Y.-Q.; Pei, J.-F.; Liu, Z.-M.; Lai, L.-H.; Cui, J.-R.; Li, R.-T. *Bioorg. Med. Chem.* **2006**, *14*, 1483-1496.
19. Lindsten, K.; Menendez-Benito, V.; Masucci, M.G.; Dantuma, N.P. *Nat. Biotechnol.* **2003**, *21*, 897-902.
20. Adams, J.; Behnke, M.; Chen, S.; Cruickshank, A. A.; Dick, L. R.; Grenier, L.; Klunder, J. M.; Ma, Y.-T.; Plamondon, L.; Stein, R. L. *Bioorg. Med. Chem. Lett.* **1998**, *8*, 333-338.
21. Sin, N.; Kim, K.B.; Elofsson, M.; Meng, L.; Auth, H.; Kwok, B.H.; Crews, C.M. *Bioorg. Med. Chem. Lett.* **1999**, *9*, 2283-2288.
22. Kaiser, E.; Colescott, R.L.; Bossinger, C.D.; Cook, P.I. *Anal. Biochem.* **1970**, *34*, 595-598.

